Available online at www.sciencedirect.com
SCIENCE DIRECT®
Journal of Chromatography A, 1081 (2005) 163–173
JOURNAL OF CHROMATOGRAPHY A
www.elsevier.com/locate/chroma

Characterization of immobilized artificial membrane (IAM) and XTerra columns by means of chromatographic models

Elisabet Lázaro, Clara Ràfols, Martí Rosés *

Departament de Química Analítica, Universitat de Barcelona, Diagonal 647, E-08028 Barcelona, Spain

Received 19 December 2004; received in revised form 17 May 2005; accepted 23 May 2005

Abstract

Immobilized artificial membranes (IAMs) prepared from phosphatidylcholine analogs are used as stationary phases in liquid chromatography systems to model drug partitioning between an aqueous phase (mobile phase) and a cell membrane (IAM column). Two different chromatographic models, which describe retention as a function of solute and column-mobile phase properties, have been applied to characterization of an IAM and two reversed phase C18 columns (Waters XTerra MSC18 and XTerra RP18) with acetonitrile–water mobile phases. The comparison of the results shows that the phosphatidylcholine group makes IAM column more polar than both XTerra columns, specially in terms of hydrogen-bond acceptor ability. XTerra RP18 is slightly more polar than XTerra MSC18 because of the presence of the embedded carbamate polar group.
© 2005 Elsevier B.V. All rights reserved.

Keywords: Immobilized artificial membranes; XTerra columns; HPLC; LSER model; Polarity model

1. Introduction

Immobilized artificial membranes (IAMs) were developed by Pidgeon and Venkataram [1] by covalent binding of a phospholipids monolayer (typically phosphatidylcholine-PC) to silica-propylamine particles. Because of steric hindrance, some residual free propylamino groups still remain on the silica surface after coupling with the phosphatidylcholine molecules. As a result, IAM columns show a basic IAM.PC subsurface [2].

IAM columns are mainly used for the estimation of biomembrane transport properties due to the fact that they are physically and chemically similar to cell membranes and, therefore, mimic fluid phospholipid bilayers. Thus, for instance, the retention factor on IAM columns correlated well with solute partition coefficients in fluid liposome systems [3,4] and has been used to predict drug transport across the blood–brain barrier [5,6]; to prognosticate skin permeability and skin partition coefficients [7,8] and to predict intestinal absorption [3,9,10].

There is not a universal model to characterize chromatographic columns due to the fact that the retention process is very complex and depends on many factors. One of the models tested lately is a solvation parameter model [11–13]. However, there are many others which have been developed to predict the retention of a solute in RPLC. The main purpose of this work is to characterize several columns by means of two chromatographic models: the global linear solvation energy relationship (LSER) model and the polarity model. In addition to IAM.PC.DD2 column, in this report XTerra MSC18 and XTerra RP18 columns have also been tested, and all of them have been compared.

2. Theory

2.1. Linear solvent strength theory (LSST)

The retention data ($\log k$) of a neutral solute can be related to the composition of the mobile phase by means of a quasi-linear function [14–17], over a limited range of organic solvent:

$$\log k = \log k_w - m_k\phi \quad (1)$$

* Corresponding author. Tel.: +34 934039275; fax: +34 934021233.
E-mail address: marti@apolo.qui.ub.es (M. Rosés).

0021-9673/$ – see front matter © 2005 Elsevier B.V. All rights reserved.
doi:10.1016/j.chroma.2005.05.048

where k is the solute retention factor at a specific mobile phase composition, ϕ is the mobile phase composition expressed as the volume fraction of the organic modifier, k_w is the solute retention factor extrapolated to mobile phase equivalent to pure water, and m_k is a solute-dependent solvent strength parameter specific to the organic modifier on the stationary phase under consideration.

The value of k_w varies substantially with the type of mobile phase modifier, which should not vary if the Eq. (1) was valid over the entire range of mobile phase composition. Another problem of this model is that it is only valid for one solute, since different solutes require different k_w and m_k parameters.

2.2. Linear solvation energy relationship (LSER)

The LSER model has been widely used for a lot of different systems, including many chromatographic systems. The logarithmic retention factors ($\log k$) at a single mobile phase composition can be correlated with the solutes molecular properties using the LSER model [18–20]:

$$\log k = c + eE + sS + aA + bB + vV \quad (2)$$

where k is the solute retention factor. The solute descriptors are the excess molar refraction E, the dipolarity/polarizability S, the solute's effective hydrogen-bond acidity A and hydrogen-bond basicity B and McGowan's characteristic volume V.

The coefficients in Eq. (2), which are calculated by multiple linear regression, represent the difference in solvation properties of both phases forming the chromatographic system. The e coefficient depends on the difference in capacity of the solvated stationary and mobile phases to interact with solute n- or π- electrons; s is a measure of the difference in capacity of the solvated phases to take part in dipole–dipole and dipole–induced dipole interactions; the a and b coefficients represent the differences in hydrogen-bond basicity and acidity, respectively, between the stationary and the mobile phases; and v is a measure of the relative ease of forming a cavity for the solute in the solvated stationary and mobile phases.

Each mobile phase composition is characterized by a different LSER equation. Therefore, the number of retention measurements increases with the number of mobile phase compositions being characterized.

2.3. The global LSER model

It would be much more efficient if we could predict retention for multiple neutral solutes at multiple mobile phase compositions. For this reason, the LSER and LSST models were both combined [16,17]. The log k_w and m_k parameters were modelled by the LSER theory, as shown by the following equations:

$$\log k_w = c_w + e_w E + s_w S + a_w A + b_w B + v_w V \quad (3)$$

$$m_k = c_m + e_m E + s_m S + a_m A + b_m B + v_m V \quad (4)$$

Replacing Eqs. (3) and (4) in Eq. (1), a global linear solvation energy relationship model (global LSER) was derived:

$$\log k = (c_w - c_m\phi) + (e_w - e_m\phi)E + (s_w - s_m\phi)S + (a_w - a_m\phi)A + (b_w - b_m\phi)B + (v_w - v_m\phi)V \quad (5)$$

It is also possible to obtain the same model considering the coefficients of Eq. (2) as linear relationships of ϕ. The global LSER is a great experimental simplification, since it only requires 12 coefficients instead of six coefficients for every ϕ value using the LSER model.

2.4. The polarity model

We have developed a polarity model for neutral solutes [17,21] based on a new solvent parameter (P_m^N), which is related to acetonitrile–water mobile phase composition:

$$P_m^N = 1.00 - \frac{2.13\phi}{1 + 1.42\phi} \quad (6)$$

The retention factors in all experimental mobile phases are related to this parameter, according to:

$$\log k = q + pP_m^N \quad (7)$$

where q and p are constants depending on the solute. Next, a linear correlation is established between q and p for all solutes in order to obtain first estimates of $(\log k)_0$ and P_s^N parameters:

$$q = (\log k)_0 - pP_s^N \quad (8)$$

Replacing Eq. (8) in Eq. (7) leads to the following equation:

$$\log k = (\log k)_0 + p(P_m^N - P_s^N) \quad (9)$$

where p is a solute parameter, P_m^N is a mobile phase parameter and $(\log k)_0$ and P_s^N are two stationary phase constant parameters. Nevertheless, these values can be improved in an iterative process by minimising the sum of squared residuals (SSR) between the predicted and the experimental $\log k$. After a few iterations, we obtain not only the optimal $(\log k)_0$ and P_s^N parameters, but also refinated p values [22].

3. Experimental

3.1. Apparatus

The retention data were measured in an IAM.PC.DD2 column (100 mm × 4.6 mm I.D., 12 μm, Regis Technologies Inc., Morton Grove, IL, USA), XTerra MSC18 and XTerra RP18 columns (150 mm × 4.6 mm I.D., 5 μm, Waters Corporation, Milford, MA, USA). All measurements were

performed with a Shimadzu liquid chromatograph (Kyoto, Japan) equipped with two Shimadzu LC-10AD pumps and a Shimadzu SPD-10AV detector. The temperature was controlled at 25.0 ± 0.1 °C with a Shimadzu CTO-10AS column oven. All pH measurements were taken with a Ross Combination electrode Orion 8102 (glass electrode and a reference electrode with a 3.0 M KCl solution in water as salt bridge) in a Crison micropH 2002 potentiometer with a precision of ±0.1 mV (±0.002 pH units).

3.2. Chemicals

Acetonitrile was HPLC grade from Merck (Darmstadt, Germany) and water purified by the Milli-Q plus system from Millipore, with a resistivity of 18.2 MΩ cm. The sodium dihydrogenphosphate monohydrate (GR), the disodium hydrogenphosphate (GR) and the sodium hydroxide (GR) were from Merck. The test solutes employed were reagent grade or better and obtained from Merck, Fluka (Steinheim, Germany), Aldrich (Steinheim, Germany) or Carlo Erba (Milano, Italy).

3.3. Procedure

The eluents were mixtures of acetonitrile and 0.01 M phosphate aqueous buffer adjusted at pH 7, in percentages ranging from 10 to 60 % for IAM.PC.DD2 column, and from 20 to 60% for XTerra columns, due to the extremely large retention times of several solutes in these columns. All compounds were solved in methanol and their concentration were 0.1 mg mL^{-1}. The injection volume was always 10 μL. The detection wavelength was at 254 nm for all the compounds (except geraniol, alpha-pinene, pyrrole and furan, whose wavelength was at 214 nm). Isocratic conditions were always used at a flow rate of 1 mL min^{-1}. The column hold-up time was determined by using an aqueous solution of potassium bromide (0.1 mg mL^{-1}) as an unretained solute. Its detection was performed at 200 nm. Retention data were expressed by the logarithm of the capacity factor, $\log k$, defined as $\log k = \log[(t_r - t_o)/t_o]$ where t_r and t_o are the retention times of the solute and the unretained compound, respectively. All measurements were taken in triplicate.

4. Results and discussion

The retention of 59 solutes in IAM.PC.DD2, XTerra MSC18 and XTerra RP18 columns has been characterized by means of the global LSER and the polarity models. The $\log k$ values were obtained for all solutes in the different chromatographic systems. However, some compounds could not be measured in all mobile phases due to their strong retention. The retention data follow the trend expected in the reversed-phase liquid chromatography (RPLC), i.e., retention increases when the acetonitrile content of the mobile phase decreases.

4.1. Application of the global LSER model to neutral compounds

The global LSER model (Eq. (5)) is derived taking LSST and LSER models into account. The LSST model describes a linear relationship between the solute retention and the volume fraction of organic solvent, but it is only observed over a limited range of mobile phase composition. Eq. (1) was applied to the retention data of each solute at the mobile phase compositions studied in order to check if the tested mobile phase range was included in the linear range. The $\log k_w$, m_k and statistics of all solutes and columns are shown in Table 1. In general, very good correlations were obtained.

The LSER model correlates the retention data with the molecular properties of the solutes studied, whose descriptors are shown in Table 2. In order to check the applicability of the global LSER model (Eq. (5)), we correlate the solute descriptors with the $\log k_w$ and m_k parameters of Table 1. We obtained two relationships ($\log k_w$ and m_k) for each column (IAM.PC.DD2, XTerra MSC18 and XTerra RP18, respectively):

$$\log k_w = -0.572 + 0.716E - 0.843S + 0.124A - 2.317B + 2.785V \quad \mathrm{SD} = 0.102,\ r = 0.993,\ F = 639 \tag{10}$$

$$m_k = 0.555 + 0.844E - 0.941S - 0.039A - 3.035B + 3.734V \quad \mathrm{SD} = 0.177,\ r = 0.989,\ F = 450 \tag{11}$$

$$\log k_w = -0.031 + 0.312E - 0.766S - 0.456A - 3.082B + 3.533V \quad \mathrm{SD} = 0.090,\ r = 0.996,\ F = 915 \tag{12}$$

$$m_k = 0.386 + 0.608E - 0.929S - 0.123A - 3.486B + 4.215V \quad \mathrm{SD} = 0.145,\ r = 0.990,\ F = 394 \tag{13}$$

$$\log k_w = -0.213 + 0.471E - 0.720S - 0.222A - 2.991B + 3.299V \quad \mathrm{SD} = 0.076,\ r = 0.997,\ F = 1212 \tag{14}$$

$$m_k = 0.158 + 0.449E - 0.659S + 0.043A - 3.369B + 4.012V \quad \mathrm{SD} = 0.109,\ r = 0.994,\ F = 666 \tag{15}$$

After this proof, the global LSER model was applied to the retention data, and three equations were obtained (for IAM.PC.DD2, XTerra MSC18 and XTerra RP18 columns, respectively):

$$\log k = (-0.520 - 0.603\phi) + (0.758 - 0.979\phi)E + (-0.843 + 0.849\phi)S + (0.146 + 0.066\phi)A + (-2.199 + 2.787\phi)B + (2.644 - 3.426\phi)V \quad \mathrm{SD} = 0.096,\ r = 0.992,\ F = 1153 \tag{16}$$

$$\log k = (0.002 - 0.505\phi) + (0.423 - 0.746\phi)E + (-0.811 + 0.803\phi)S + (-0.400 + 0.132\phi)A + (-3.094 + 3.338\phi)B + (3.419 - 3.738\phi)V$$
$$\mathrm{SD} = 0.092,\ r = 0.993,\ F = 902 \quad (17)$$

$$\log k = (-0.219 - 0.192\phi) + (0.470 - 0.615\phi)E + (-0.584 + 0.494\phi)S + (-0.248 + 0.060\phi)A + (-3.003 + 3.317\phi)B + (3.180 - 3.642\phi)V$$
$$\mathrm{SD} = 0.062,\ r = 0.996,\ F = 1559 \quad (18)$$

Table 1
Correlations of log k values of the studied solutes with the mobile phase composition (ϕ) according to Eq. (1)

Solute	IAM.PC.DD2, $\log k = \log k_w - m_k\phi$					XTerra MSC18, $\log k = \log k_w - m_k\phi$					XTerra RP18, $\log k = \log k_w - m_k\phi$				
	$\log k_w$	m_k	r	SD	F	$\log k_w$	m_k	r	SD	F	$\log k_w$	m_k	r	SD	F
2,3-Benzofuran	1.496	3.702	0.944	0.352	16	2.331	3.446	0.994	0.101	93	2.141	3.208	0.998	0.064	201
2,3-Dimethylphenol	1.441	3.192	0.997	0.061	398	1.885	3.162	0.991	0.121	55	1.800	2.914	0.995	0.079	109
2,4-Dimethylphenol	1.460	3.239	0.997	0.062	404	1.929	3.248	0.992	0.116	63	1.822	2.951	0.995	0.082	103
2-Naphtol	1.933	3.880	0.994	0.114	170	2.065	3.513	0.990	0.137	52	2.137	3.471	0.992	0.125	61
2-Nitroaniline	1.125	2.893	0.999	0.037	906	1.523	2.704	0.992	0.096	63	1.486	2.527	0.997	0.055	172
2-Nitroanisole	1.088	3.016	0.999	0.031	1410	1.776	2.962	0.994	0.089	89	1.619	2.708	0.998	0.050	232
3-Chloroaniline	1.207	2.961	0.999	0.039	864	1.671	2.821	0.993	0.092	75	1.587	2.622	0.997	0.053	196
3-Nitroaniline	0.925	2.635	0.999	0.022	2052	1.334	2.514	0.997	0.052	189	1.308	2.327	0.998	0.038	302
4-Chloroacetanilide	1.267	3.110	0.994	0.090	176	1.592	3.067	0.985	0.150	34	1.553	2.855	0.988	0.124	42
4-Chloroaniline	1.156	2.892	0.998	0.042	714	1.597	2.765	0.992	0.099	63	1.495	2.548	0.996	0.061	141
4-Chlorophenol	1.541	3.269	0.997	0.071	310	1.790	3.164	0.989	0.130	47	1.768	2.944	0.994	0.089	88
4-Nitroaniline	1.012	2.752	0.997	0.052	415	1.199	2.405	0.993	0.082	70	1.277	2.360	0.997	0.049	188
Acetanilide	0.480	2.109	0.997	0.041	400	0.778	1.980	0.979	0.116	23	0.765	1.866	0.991	0.073	53
Acetophenone	0.760	2.541	0.999	0.026	1450	1.441	2.513	0.991	0.093	59	1.252	2.229	0.996	0.054	136
Aniline	0.351	1.813	0.999	0.016	1846	1.785	3.589	0.948	0.341	9	0.671	1.481	1.000	0.010	1740
Anisole	1.062	2.826	0.999	0.020	3081	1.904	2.897	0.996	0.071	134	1.661	2.581	0.999	0.034	471
Antipyrine	0.222	1.827	0.991	0.068	108	0.577	2.025	0.961	0.164	12	0.387	1.651	0.963	0.131	13
Benzaldehyde	0.630	2.252	0.999	0.014	3842	1.307	2.307	0.996	0.057	132	1.140	2.029	0.999	0.031	333
Benzamide	0.121	1.593	0.995	0.045	189	−0.009	0.962	0.999	0.011	616	0.275	1.404	0.983	0.074	28
Benzene	0.955	2.542	0.998	0.043	511	1.836	2.656	0.998	0.047	256	1.610	2.420	1.000	0.014	2292
Benzophenone	2.063	4.295	0.996	0.097	291	2.906	4.307	0.993	0.145	71	2.675	3.991	0.994	0.128	78
Benzonitrile	0.767	2.477	0.999	0.015	3874	1.478	2.500	0.996	0.064	121	1.318	2.251	0.999	0.031	426
Benzyl benzoate	2.706	5.276	0.996	0.124	267	–	–	–	–	–	–	–	–	–	–
Bromobenzene	1.748	3.564	0.998	0.049	773	2.580	3.600	0.996	0.087	137	2.378	3.402	0.997	0.075	163
Butylbenzene	2.784	5.035	0.995	0.143	100	–	–	–	–	–	–	–	–	–	–
Butyrophenone	1.561	3.591	0.998	0.056	605	2.490	3.651	0.993	0.120	74	2.253	3.388	0.996	0.090	114
Caffeine	−0.166	1.291	0.964	0.097	26	−0.052	1.001	0.907	0.131	5	−0.071	0.884	0.967	0.066	14
Chlorobenzene	1.584	3.384	0.999	0.041	982	2.416	3.396	0.997	0.072	178	2.235	3.235	0.997	0.065	199
Corticosterone	1.694	3.951	0.982	0.205	55	1.251	2.385	0.999	0.015	2013	2.093	4.020	0.970	0.287	16
Cortisone	1.294	3.584	0.982	0.188	53	1.895	4.032	0.960	0.333	12	1.696	3.616	0.969	0.259	15
Estradiol	2.652	4.557	0.984	0.234	30	–	–	–	–	–	–	–	–	–	–
Estriol	1.658	3.406	0.985	0.160	67	1.508	3.643	0.963	0.286	13	1.859	3.933	0.969	0.284	15
Ethylbenzene	1.805	3.713	0.999	0.046	949	2.843	3.823	0.996	0.092	139	2.541	3.567	0.998	0.058	307
Furan	0.322	1.732	0.994	0.050	180	1.095	1.829	0.999	0.009	3676	0.935	1.623	0.999	0.022	430
Geraniol	1.799	3.999	0.979	0.224	47	2.753	4.299	0.985	0.211	33	2.452	3.943	0.989	0.163	47
Heptanophenone	2.985	5.492	0.996	0.123	292	–	–	–	–	–	–	–	–	–	–
Hydrocortisone	1.303	3.371	0.977	0.201	42	1.517	3.384	0.967	0.253	14	1.656	3.572	0.964	0.278	13
m-Cresole	1.050	2.685	0.997	0.049	435	1.428	2.657	0.990	0.106	50	1.352	2.404	0.996	0.058	139
Methyl benzoate	1.106	2.959	0.999	0.032	1233	1.930	3.041	0.991	0.112	59	1.694	2.725	0.996	0.068	130
Monuron	1.237	3.166	0.995	0.086	198	1.606	3.077	0.986	0.145	36	1.548	2.862	0.989	0.119	46
Myrcene	3.014	5.370	0.995	0.149	104	–	–	–	–	–	–	–	–	–	–
Naphthalene	2.149	4.169	0.997	0.078	423	2.941	4.096	0.994	0.123	89	2.733	3.898	0.996	0.103	114
Nitrobenzene	1.040	2.796	0.999	0.020	2901	1.751	2.784	0.996	0.065	148	1.581	2.526	0.999	0.027	708
o-Toluidine	0.645	2.208	0.999	0.014	3729	0.774	1.408	0.985	0.070	32	1.039	1.926	0.998	0.032	293
Phenol	0.687	2.202	0.999	0.025	1142	0.964	2.053	0.992	0.073	63	0.952	1.898	0.998	0.034	246
Propiophenone	1.161	3.048	0.999	0.038	942	2.103	3.303	0.989	0.141	44	1.758	2.786	0.997	0.064	150
Propylbenzene	2.287	4.359	0.998	0.064	682	–	–	–	–	–	–	–	–	–	–
p-Xylene	1.834	3.728	0.999	0.045	1015	2.865	3.862	0.996	0.088	152	2.540	3.547	0.998	0.057	308
Pyrimidine	−0.499	0.597	0.994	0.017	175	−0.509	0.181	0.881	0.027	3	−0.467	0.184	0.872	0.029	3
Pyrocatechol	0.487	1.768	0.998	0.028	584	0.446	1.544	0.983	0.081	29	0.466	1.435	0.996	0.036	127
Pyrrole	0.177	1.505	0.995	0.040	211	0.589	1.341	1.000	0.000	1.5E+7	0.538	1.209	0.996	0.029	138
Quinoline	2.065	4.303	0.996	0.096	296	1.711	3.201	0.963	0.253	13	1.204	2.360	0.986	0.114	34
Resorcinol	0.396	1.787	0.994	0.054	160	0.224	1.369	0.984	0.069	31	0.338	1.410	0.994	0.042	89
Thiourea	−0.615	0.309	0.993	0.010	152	−1.297	0.513	0.851	0.090	3	−1.390	0.746	0.967	0.055	14
Thymol	2.194	4.267	0.997	0.086	363	2.883	4.319	0.992	0.149	68	2.717	4.018	0.995	0.110	106
Toluene	1.401	3.147	0.999	0.035	1167	2.331	3.239	0.998	0.058	248	2.107	3.049	0.998	0.049	304
Valerophenone	2.010	4.191	0.998	0.073	482	3.037	4.298	0.994	0.133	83	2.752	3.989	0.995	0.113	100

Table 2
Solute descriptors studied in this work

Solute	*E*	*S*	*A*	*B*	*V*
2,3-Benzofuran	0.888	0.83	0.00	0.15	0.9053
2,3-Dimethylphenol	0.850	0.90	0.52	0.36	1.0569
2,4-Dimethylphenol	0.840	0.80	0.53	0.39	1.0569
2-Naphtol	1.520	1.08	0.61	0.40	1.1441
2-Nitroaniline	1.180	1.37	0.30	0.36	0.9904
2-Nitroanisole	0.968	1.34	0.00	0.38	1.0902
3-Chloroaniline	1.050	1.10	0.30	0.36	0.9390
3-Nitroaniline	1.200	1.71	0.40	0.35	0.9904
4-Chloroacetanilide	0.980	1.50	0.64	0.51	1.2357
4-Chloroaniline	1.060	1.10	0.30	0.35	0.9390
4-Chlorophenol	0.915	1.08	0.67	0.20	0.8975
4-Nitroaniline	1.220	1.91	0.42	0.38	0.9904
Acetanilide	0.870	1.36	0.46	0.69	1.1137
Acetophenone	0.818	1.01	0.00	0.48	1.0139
Alpha-pinene	0.446	0.14	0.00	0.12	1.2574
Aniline	0.955	0.96	0.26	0.50	0.8162
Anisole	0.708	0.75	0.00	0.29	0.9160
Antipyrine	1.320	1.50	0.00	1.48	1.5502
Benzaldehyde	0.820	1.00	0.00	0.39	0.8730
Benzamide	0.990	1.50	0.49	0.67	0.9728
Benzene	0.610	0.52	0.00	0.14	0.7164
Benzophenone	1.447	1.50	0.00	0.50	1.4808
Benzonitrile	0.742	1.11	0.00	0.33	0.8711
Benzyl benzoate	1.264	1.42	0.00	0.51	1.6804
Bromobenzene	0.882	0.73	0.00	0.09	0.8914
Butylbenzene	0.600	0.51	0.00	0.15	1.2800
Butyrophenone	0.797	0.95	0.00	0.51	1.2957
Caffeine	1.500	1.60	0.00	1.33	1.3632
Chlorobenzene	0.718	0.65	0.00	0.07	0.8388
Corticosterone	1.860	3.43	0.40	1.63	2.7389
Cortisone	1.960	3.50	0.36	1.87	2.7546
Dodecanophenone	0.720	0.95	0.00	0.50	2.4229
Estradiol	1.800	3.30	0.88	0.95	2.1988
Estriol	2.000	3.36	1.40	1.22	2.2575
Ethylbenzene	0.613	0.51	0.00	0.15	0.9982
Furan	0.369	0.53	0.00	0.13	0.5363
Geraniol	0.513	0.63	0.39	0.66	1.4903
Heptanophenone	0.720	0.95	0.00	0.50	1.7184
Hydrocortisone	2.030	3.49	0.71	1.90	2.7975
m-Cresole	0.822	0.88	0.57	0.34	0.9160
Methyl benzoate	0.733	0.85	0.00	0.46	1.0726
Monuron	1.140	1.50	0.47	0.78	1.4768
Myrcene	0.483	0.29	0.00	0.21	1.0000
Naphthalene	1.340	0.92	0.00	0.20	1.0854
Nitrobenzene	0.871	1.11	0.00	0.28	0.8906
o-Toluidine	0.970	0.90	0.23	0.59	0.9571
Phenol	0.805	0.89	0.60	0.30	0.7751
Propiophenone	0.804	0.95	0.00	0.51	1.1548
Propylbenzene	0.604	0.50	0.00	0.15	1.1391
p-Xylene	0.613	0.52	0.00	0.16	0.9982
Pyrimidine	0.606	1.00	0.00	0.65	0.6342
Pyrocatechol	0.970	1.10	0.88	0.47	0.8338
Pyrrole	0.613	0.73	0.41	0.29	0.5774
Quinoline	1.268	0.97	0.00	0.51	1.0443
Resorcinol	0.980	1.00	1.10	0.58	0.8338
Thiourea	0.840	0.82	0.77	0.87	0.5696
Thymol	0.822	0.79	0.52	0.44	1.3387
Toluene	0.601	0.52	0.00	0.14	0.8573
Valerophenone	0.795	0.95	0.00	0.50	1.4366

The coefficients of Eqs. (16)–(18), which are multiplying to the capital letters, correspond to the same coefficients shown in Eq. (2), but represented as a linear relationship of ϕ. Positive coefficients imply an increase in $\log k$, i.e., partition into the stationary phase is favoured. For the same reason, negative coefficients mean that partition into the mobile phase is favoured. The larger the coefficient absolute value, the greater the influence on the retention in RPLC.

For all columns studied, b and v coefficients have the largest absolute values. The v coefficient is large and positive in all cases and its value increases with the water content in the mobile phase. This fact is due to the cohesive density of water. Therefore, creating a cavity inside the mobile phase requires more energy than the necessary in the stationary phase. All b coefficients are large and negative, which indicates that the hydrogen-bond acidity of the stationary phase is lower than the hydrogen-bond acidity of the mobile phase. Therefore, solutes with greater hydrogen-bond acceptor ability (large B descriptor value) are less retained.

All columns have negative s coefficient values, which shows that they are less dipolar than the mobile phase. Regarding the e coefficient, all columns have positive values, which indicates that they are more polarizable than mobile phase.

The solute hydrogen-bond basicity term (a coefficient) depends on the column. Both XTerra columns have a negative values; therefore, they are worse hydrogen-bond acceptors than mobile phase. However, the IAM.PC.DD2 column has a positive a coefficient, which indicates that this stationary phase is more hydrogen-bond basic than mobile phase.

The global LSER model for neutral compounds requires 12 mobile–stationary phase parameters (c_w, c_m, e_w, e_m, s_w, s_m, a_w, a_m, b_w, b_m, v_w, v_m) and five solute parameters (E, S, A, B, V) [16].

4.2. Application of the polarity model to neutral compounds

The polarity model relates the retention factor (k) of a neutral compound with a solute parameter (p), a mobile phase parameter (P_m^N) and two stationary phase constant parameters ($(\log k)_0$ and P_s^N) [21]. In order to obtain first estimations of p values, $\log k$ values were correlated with P_m^N for each solute according to Eq. (7).

Next, q versus p values were represented to achieve initial $(\log k)_0$ and P_s^N parameters, according to Eq. (8) (see Fig. 1). These parameters were respectively (−0.940, 0.172) for IAM.PC.DD2 column, (−1.102, −0.027) for XTerra MSC18 column and (−0.905, 0.013) for XTerra RP18 column. In order to improve these parameters, two or three iterations were done for each column [22]. The best fitting parameters are represented in the following equations:

$$\log k = -0.982 + p(P_m^N - 0.154)$$
$$\mathrm{SD} = 0.071,\ r = 0.996,\ F = 25059 \qquad (19)$$

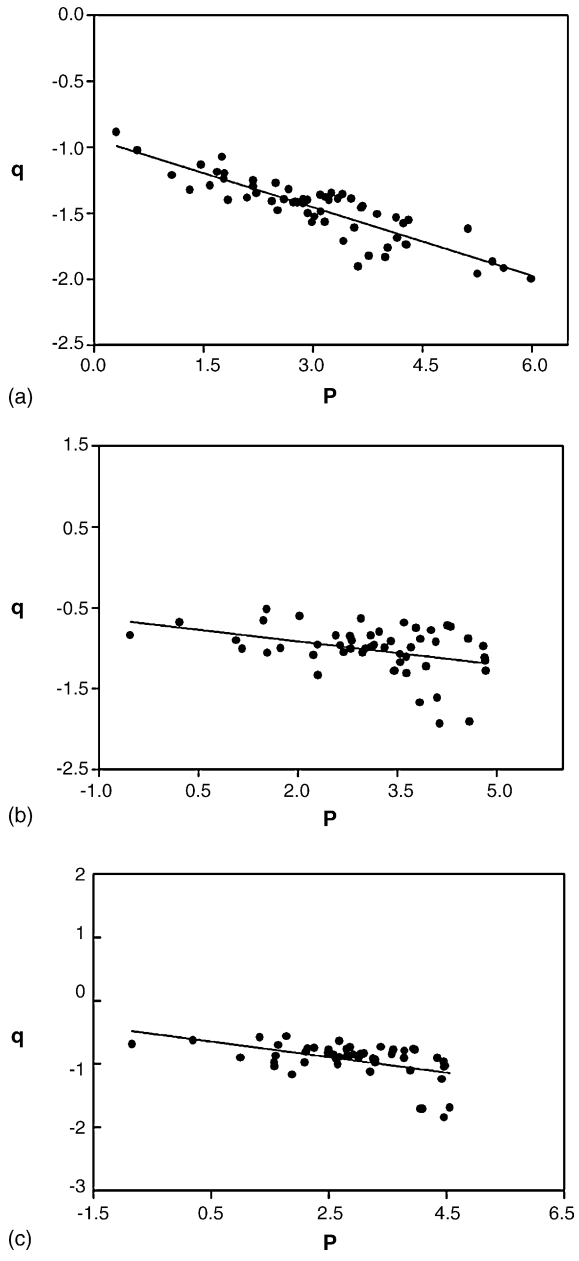

Fig. 1. Plot of q vs. p parameters for all solutes and columns tested: (a) IAM.PC.DD2, (b) XTerra MSC18 and (c) XTerra RP18 column.

$$\log k = -0.992 + p(P_m^N + 0.010)$$
$$\mathrm{SD} = 0.058,\ r = 0.997,\ F = 22062 \qquad (20)$$

$$\log k = -0.813 + p(P_m^N - 0.022)$$
$$\mathrm{SD} = 0.048,\ r = 0.997,\ F = 26075 \qquad (21)$$

for IAM.PC.DD2, XTerra MSC18 and XTerra RP18 columns, respectively. The $(\log k)_0$ parameter is the retention of any solute in a hypothetical mobile phase with the same polarity as that in the stationary phase ($P_m^N = P_s^N$), whereas the p value represents the ability of the solute to interact with

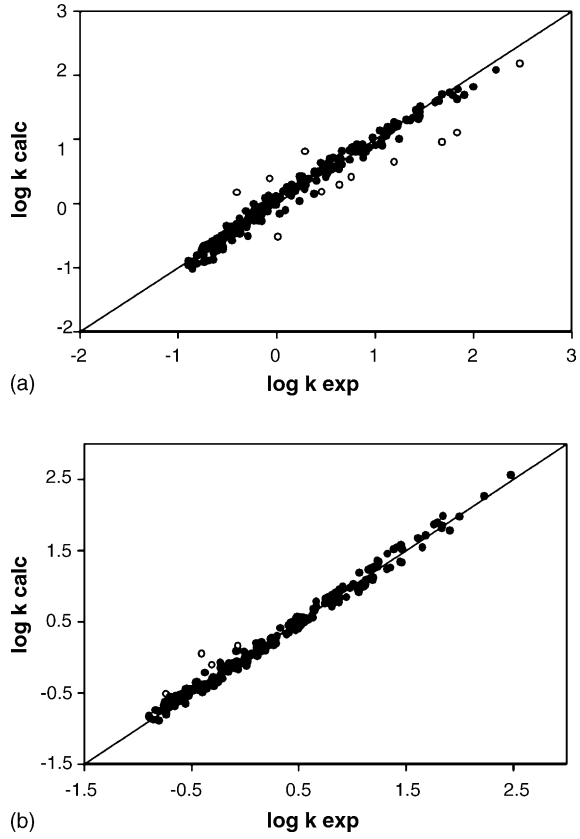

Fig. 2. Plot of calculated log *k* with the global LSER model (a) or the polarity model (b) vs. experimental log *k* for all solutes and mobile phase compositions studied in IAM.PC.DD2 column. Symbols: (●) solutes used to construct the models, (◯) outliers.

both phases. The *p* values were also improved by means of the iterative process, and are shown in Table 3.

4.3. Comparison of all columns and models studied

The plots calculated log *k* versus experimental log *k* for all columns and models are presented in Figs. 2–4. The outliers (solutes with a standard residual >|2.5|) were removed when the models were calculated, but they are also represented (by empty circles). The theoretical line with slope 1 and intercept 0 is also represented for each plot.

4.3.1. Comparison of the global LSER model with the polarity model

It has been possible to apply successfully both models to the three studied columns. The main difference between models is that Eq. (5) requires five solute parameters and twelve mobile–stationary phase parameters. Therefore, the polarity model is simpler than the global LSER model, since it requires less parameters. For this reason, it can be easier to implement it in RPLC retention prediction. However, the global LSER model characterizes better the solute–solvent interactions in the RPLC system and therefore provides more chemical information.

Table 3
Refinated *p* values for all solutes and columns

Solute	*p* (Solute polarity parameter)		
	IAM.PC.DD2	XTerra MSC18	XTerra RP18
2,3-Benzofuran	3.413	3.971	3.655
2,3-Dimethylphenol	3.357	3.321	3.182
2,4-Dimethylphenol	3.374	3.347	3.199
2-Naphtol	4.025	3.430	3.467
2-Nitroaniline	2.862	2.943	2.823
2-Nitroanisole	2.729	3.248	2.963
3-Chloroaniline	2.993	3.144	2.960
3-Nitroaniline	2.581	2.713	2.608
4-Chloroacetanilide	3.049	2.837	2.734
4-Chloroaniline	2.925	3.042	2.828
4-Chlorophenol	3.523	3.143	3.098
4-Nitroaniline	2.703	2.532	2.524
Acetanilide	1.938	2.022	1.849
Acetophenone	2.296	2.916	2.564
Aniline	1.813	2.375	1.925
Anisole	2.765	3.529	3.134
Antipyrine	1.554	1.618	1.248
Benzaldehyde	2.169	2.799	2.479
Benzamide	1.460	1.212	1.195
Benzene	2.681	3.560	3.143
Benzophenone	4.086	4.487	4.179
Benzonitrile	2.339	2.991	2.680
Benzyl benzoate	4.919	–	–
Bromobenzene	3.794	4.337	3.993
Butylbenzene	5.443	–	–
Butyrophenone	3.410	4.135	3.754
Caffeine	1.035	1.109	0.865
Chlorobenzene	3.549	4.163	3.824
Corticosterone	3.520	2.640	–
Cortisone	3.022	–	–
Estradiol	5.512	–	–
Estriol	3.695	4.140	–
Ethylbenzene	3.838	4.685	4.203
Furan	1.794	2.712	2.350
Geraniol	3.790	4.207	3.770
Heptanophenone	5.372	–	–
Hydrocortisone	3.009	1.962	–
m-Cresole	2.813	2.798	2.642
Methyl benzoate	2.792	3.560	3.101
Monuron	2.964	2.856	2.719
Myrcene	5.753	–	–
Naphthalene	4.316	4.688	4.356
Nitrobenzene	2.734	3.317	3.013
o-Toluidine	2.221	2.729	2.350
Phenol	2.310	2.322	2.196
Propiophenone	2.862	3.639	3.186
Propylbenzene	4.500	–	–
p-Xylene	3.889	4.700	4.215
Pyrimidine	0.689	0.788	0.558
Pyrocatechol	2.113	1.686	1.552
Pyrrole	1.611	2.084	1.846
Quinoline	4.087	3.117	2.381
Resorcinol	1.904	1.384	1.314
Thiourea	0.590	−0.233	−0.635
Thymol	4.360	4.434	4.243
Toluene	3.292	4.107	3.697
Valerophenone	4.027	4.737	4.332

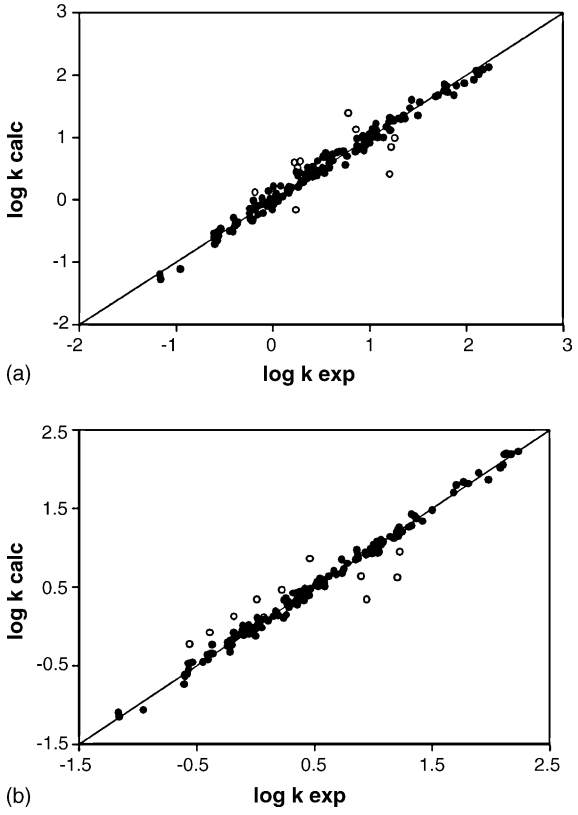

Fig. 3. Plot of calculated log k with the global LSER model (a) or the polarity model (b) vs. experimental log k for all solutes and mobile phase compositions studied in XTerra MSC18 column. Symbols: (●) solutes used to construct the models, (◯) outliers.

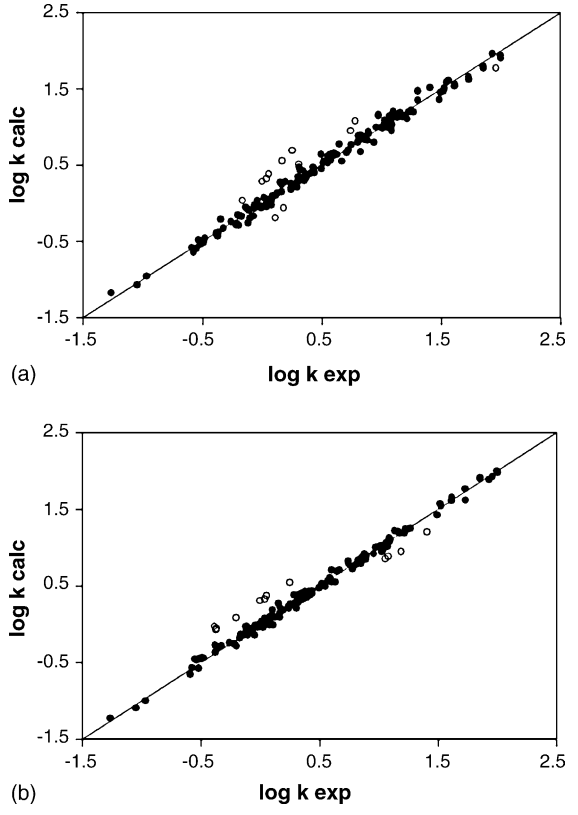

Fig. 4. Plot of calculated log k with the global LSER model (a) or the polarity model (b) vs. experimental log k for all solutes and mobile phase compositions studied in XTerra RP18 column. Symbols: (●) solutes used to construct the models, (◯) outliers.

Plots of calculated log k (with each model) versus experimental log k for all solutes, mobile phase compositions and columns are shown in Figs. 2–4. For IAM.PC.DD2 column, we can compare its plots and its respective correlations:

$$\log k \text{ calc} = 0.003 + 0.984 \log k \text{ exp}$$
$$n = 222,\ \text{SD} = 0.093,\ r = 0.992,\ F = 13288 \qquad (22)$$

which corresponds to Fig. 2a and:

$$\log k \text{ calc} = 0.002 + 0.991 \log k \text{ exp}$$
$$n = 225,\ \text{SD} = 0.071,\ r = 0.996,\ F = 24830 \qquad (23)$$

for Fig. 2b. The statistics of both correlations are very similar, but they are slightly better for the polarity model. The same can be observed for XTerra MSC18. The correlation of Fig. 3a is:

$$\log k \text{ calc} = 0.007 + 0.986 \log k \text{ exp}$$
$$n = 156,\ \text{SD} = 0.088,\ r = 0.993,\ F = 10615 \qquad (24)$$

which should be compared with the correlation of Fig. 3b:

$$\log k \text{ calc} = 0.003 + 0.994 \log k \text{ exp}$$
$$n = 142,\ \text{SD} = 0.058,\ r = 0.997,\ F = 22062 \qquad (25)$$

Moreover, both models show very good fitting for XTerra RP18 column. The correlation of Fig. 4a is:

$$\log k \text{ calc} = 0.004 + 0.992\ \log k\ \text{exp}$$
$$n = 151,\ \text{SD} = 0.060,\ r = 0.996,\ F = 18383 \qquad (26)$$

which we compare with the correlation of Fig. 4b:

$$\log k \text{ calc} = 0.002 + 0.995 \log k \text{ exp}$$
$$n = 141,\ \text{SD} = 0.048,\ r = 0.997,\ F = 26075 \qquad (27)$$

Therefore, we must conclude that both models predict retention with a similar accuracy.

4.3.2. *Comparison of the studied columns*

The structures of all stationary phases are presented in Figs. 6–8 and their main characteristics are shown in Table 4. The XTerra columns are longer and have a surface area and bonding density higher than those of the IAM.PC.DD2 column, thus they have more stationary phase that can interact with solutes. Therefore, all compounds are less retained in the IAM.PC.DD2 column, which shows shorter retention times.

On the other hand, the chemical properties of the studied columns can be compared by examining the coefficients of Eqs. (16)–(18). The most hydrophobic stationary phase

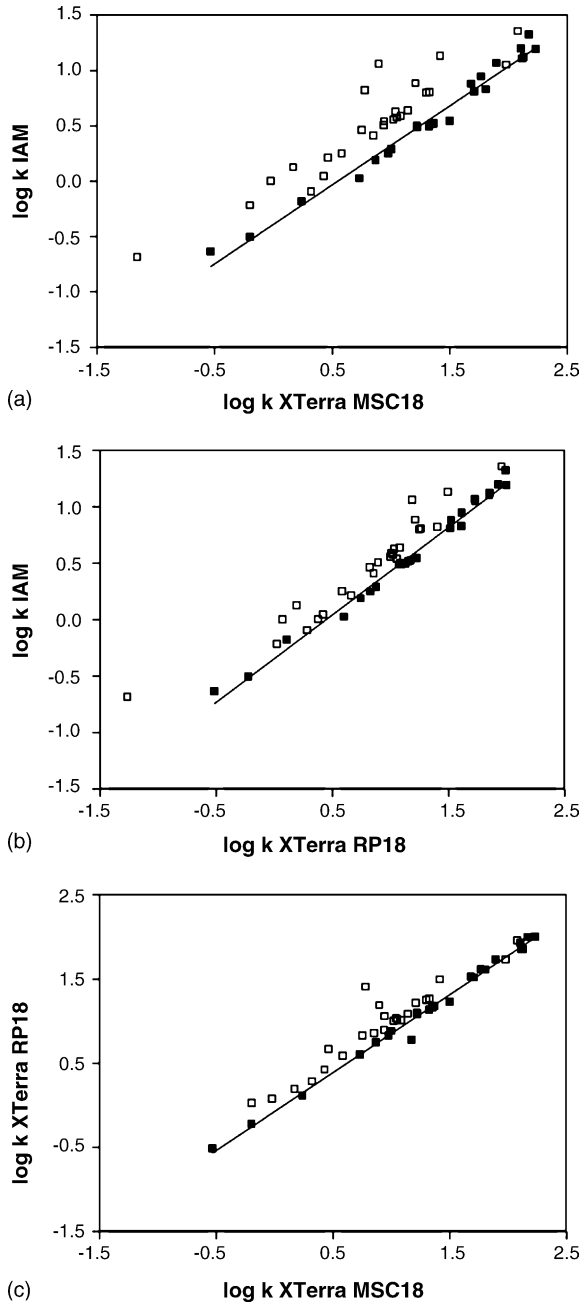

Fig. 5. Plots of experimental log k in: IAM.PC.DD2 column versus XTerra MSC18 column (a) or XTerra RP18 column (b), and experimental log k in XTerra RP18 column versus XTerra MSC18 column (c). Symbols: (■) solutes with $A = 0$, (□) solutes with $A > 0$.

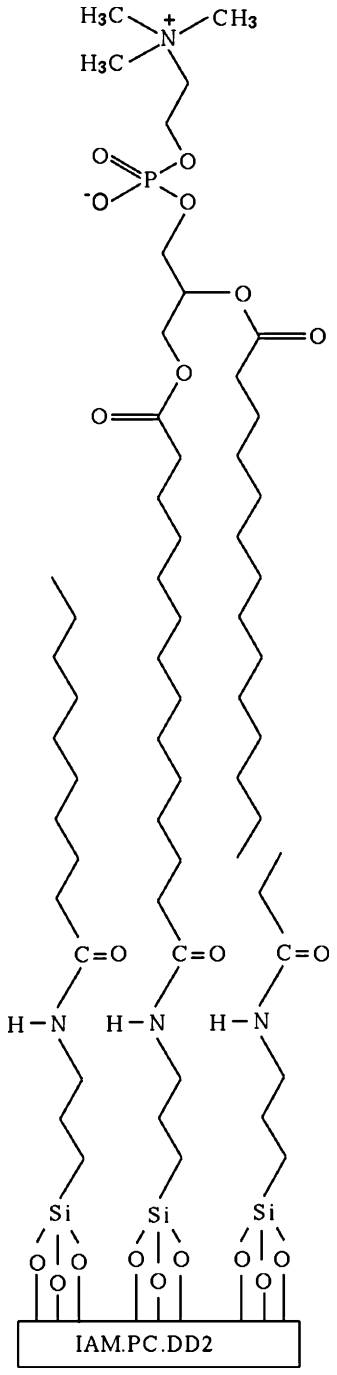

Fig. 6. Structure of studied IAM.PC.DD2 stationary phase.

Table 4
Characteristics of columns used in the present study

Column	Dimensions (mm)	Particle size (μm)	Pore diameter (Å)	Surface area (m^2/g)	Bonding density (μmol/m^2)
IAM.PC.DD2	100 × 4.6	12	300	120	0.66 (C(iam)) 0.52 (C_{10}/C_3)
XTerra MSC18	150 × 4.6	5	125	179	2.14 (C_{18})
XTerra RP18	150 × 4.6	5	127	178	2.28 (C_{18})

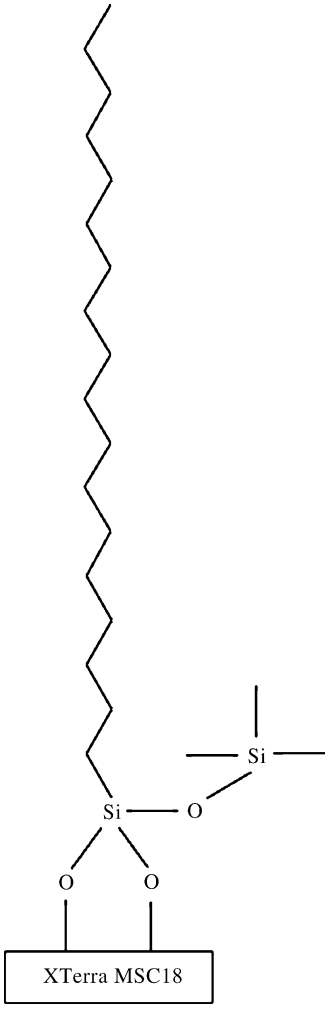

Fig. 7. Structure of studied XTerra MSC18 stationary phase.

(the largest v coefficient) is XTerra MSC18, and the least one is IAM.PC.DD2. XTerra RP18 column has an intermediate hydrophobicity between the two other columns. As regards a coefficient, IAM.PC.DD2 has the largest positive value; therefore it would become the most hydrogen-bond basic of the columns studied. XTerra RP18 goes behind it, and next, XTerra MSC18. The hydrogen-bond acidity (b coefficient) follows the same order. Regarding the e coefficient, IAM.PC.DD2 column is the most polarizable system, and XTerra RP18 is slightly more polarizable than XTerra MSC18.

However, from among all coefficients described above, the most important differences are shown by coefficient a, whereas the other coefficients are quite similar. This means that solutes without hydrogen-bond acidity ($A = 0$) should behave similarly in all columns, whereas hydrogen-bond acids ($A > 0$) should show retention differences. In order to prove the different hydrogen-bond acceptor ability of each column, plots of retention data of each tested column versus the other two at 20% of acetonitrile were constructed separately (Fig. 5). All solutes were divided

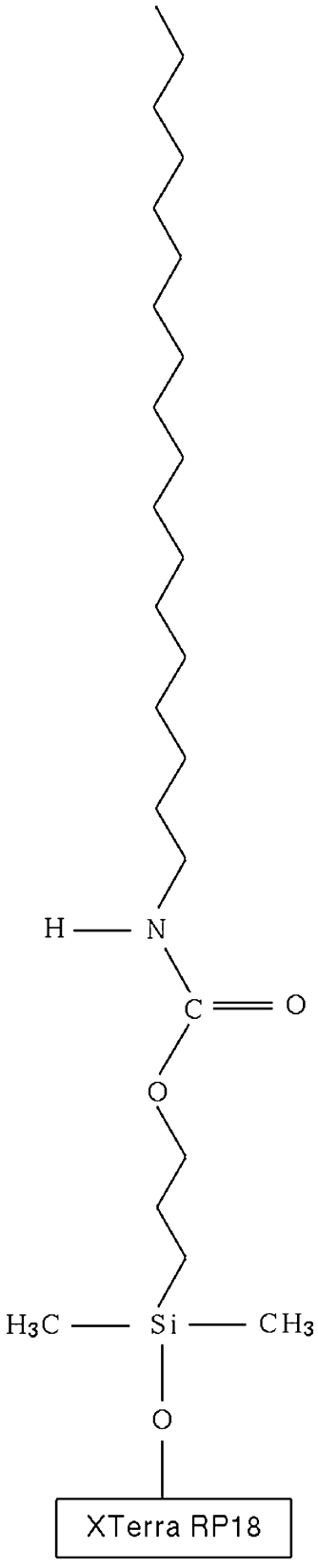

Fig. 8. Structure of studied XTerra RP18 stationary phase.

into two groups. Those compounds represented by a full square have a descriptor $A = 0$, whereas the empty squares show solutes with $A > 0$. Due to the great hydrogen-bond acceptor ability of IAM.PC.DD2 column, hydrogen-bond donors solutes ($A > 0$) should be more retained in this column than in XTerra columns. We can appreciate clearly this trend in Fig. 5a. In contrast, XTerra RP18 column has an intermediate basicity. Consequently, the differences of data retention between solutes with $A = 0$ and $A > 0$ in relation to the other tested columns are less evidenced (see Fig. 5b,c). Taillardat- Bertschinger et al. [2] proposed that the basicity of IAM.PC.DD2 column was mainly due to the residual-free propylamino groups on the silica surface. Nevertheless, other groups such as negatively charged head group could also influence its hydrogen-bond acceptor ability. On the other hand, the intermediate basicity of XTerra RP18 column could be attributed to its embedded carbamate polar group, which behaves as hydrogen-bond acceptor. Unlike IAM.PC.DD2 column, in this column there are not residual-free propylamino groups, since the amide polar group is introduced in the bonding process to silica support in a different way [23].

The differences in stationary phase hydrogen-bond basicity should be reflected in the overall polarity of the columns, which can be measured through P_s^N parameters of Eqs. (19)–(21). The IAM.PC.DD2 column is more polar than the XTerra RP18 column, being XTerra MSC18 the least polar column.

5. Conclusions

It has been proved that it is possible to apply successfully the global LSER and polarity models to the three studied columns, and therefore, they can be considered as models with general applicability for prediction of RPLC retention in acetonitrile/water mobile phase. Regarding the polarity model, we can conclude that the IAM.PC.DD2 column is the most polar, followed by the XTerra RP18 column, while the XTerra MSC18 column is the least polar. The polarity model is easier to implement in RPLC retention prediction than the global LSER model, since it requires less solute and mobile–stationary phases parameters. However, the global LSER model characterizes better the solute–solvent interactions in the RPLC system. According to this model the IAM.PC.DD2 is the most polarizable, hydrogen-bond acid and basic of the columns tested, followed by the XTerra RP18, and finally the XTerra MSC18. Nevertheless, the IAM.PC.DD2 is the least hydrophobic stationary phase. The XTerra RP18 column has an intermediate hydrophobicity, and the XTerra MSC18 column is the most hydrophobic.

Acknowledgements

We are thankful for financial support from the Spanish Government (Project CTQ2004-00965/BQU) and the Catalan Government (2001SGR00055). E.L. was supported by a grant from the Spanish Government (AP2002-3049).

References

[1] C. Pidgeon, U.V. Venkataram, Anal. Biochem. 176 (1989) 36.
[2] A. Taillardat-Bertschinger, P.A. Carrupt, F. Barbato, B. Testa, J. Med. Chem. 46 (2003) 655.
[3] S. Ong, H. Liu, C. Pidgeon, J. Chromatogr. A 728 (1996) 113.
[4] A. Taillardat-Bertschinger, C.A.M. Martinet, P.A. Carrupt, M. Reist, G. Caron, R. Fruttero, B. Testa, Pharm. Res. 19 (2002) 729.
[5] A. Ducarme, M. Neuwels, S. Goldstein, R. Massingham, Eur. J. Med. Chem. 33 (1998) 215.
[6] A. Reichel, D.J. Begley, Pharm. Res. 15 (1998) 1270.
[7] A. Nasal, M. Sznitowska, A. Bucinski, R. Kaliszan, J. Chromatogr. A 692 (1995) 83.
[8] F. Barbato, B. Cappello, A. Miro, M.I. La Rotonda, Il Farmaco 53 (1998) 655.
[9] C. Pidgeon, S. Ong, H. Liu, X. Qiu, M. Pidgeon, A.H. Dantzig, J. Munroe, W.J. Hornback, J.S. Kasher, L. Glunz, T. Szczerba, J. Med. Chem. 38 (1995) 590.
[10] M. Genty, G. González, C. Clere, V. Desangle-Gouty, J.Y. Legendre, Eur. J. Pharm. Sci. 12 (2001) 223.
[11] K. Valko, C.M. Du, C.D. Bevan, D.P. Reynolds, M.H. Abraham, J. Pharm. Sci. 89 (2000) 1085.
[12] C. Lepont, C.F. Poole, J. Chromatogr. A 946 (2002) 107.
[13] D.M. Cimpean, C.F. Poole, Analyst 127 (2002) 724.
[14] L.R. Snyder, J.W. Dolan, J.R. Gant, J. Chromatogr. 165 (1979) 3.
[15] M.A. Quarry, R.L. Grob, L.R. Snyder, Anal. Chem. 58 (1986) 907.
[16] A. Wang, L.C. Tan, P.W. Carr, J. Chromatogr. A 848 (1999) 21.
[17] S. Espinosa, E. Bosch, M. Rosés, J. Chromatogr. A 945 (2002) 83.
[18] M.H. Abraham, G.S. Whiting, R.M. Doherty, W.J. Shuely, J. Chromatogr. 587 (1991) 229.
[19] M.H. Abraham, M. Rosés, C.F. Poole, S.K. Poole, J. Phys. Org. Chem. 10 (1997) 358.
[20] M.H. Abraham, M. Rosés, J. Phys. Org. Chem. 7 (1994) 672.
[21] E. Bosch, P. Bou, M. Rosés, Anal. Chim. Acta 299 (1994) 219.
[22] J.R. Torres-Lapasió, M.C. García-Alvarez-Coque, M. Rosés, E. Bosch, J. Chromatogr. A 955 (2002) 19.
[23] J.E. O'Gara, D.P. Walsh, B.A. Alden, P. Casellini, T.H. Walter, Anal. Chem. 71 (1999) 2992.